(1)

Quarterly Progress Report

March 1, 1994 to May 31, 1994

Visible Light Emitting Materials and Injection Devices

ONR/ARPA URI

Grant Number N00014-92-J-1895

Prepared by:

Paul H. Holloway
Department of Materials Science and Engineering
University of Florida
P.O. Box 116400
Gainesville, FL 32611
Ph: 904/392-6664; FAX: 904/392-4911
E-Mail: Internet-PHOLL@MSE.UFL.EDU

Participants:
University of Florida
Kevin Jones
Robert Park
Joe Simmons
Dept. of Materials Science and Engineering
Tim Anderson
Dept. of Chemical Engineering
Peter Zory
Dept. of Electrical Engineering
University of Colorado
Jacques Pankove
Dept. of Electrical Engineering
Columbia University
Gertrude Neumark
Dept. of Materials Science and Engineering
Oregon Graduate Institute of Science and Engineering
Reinhart Engelmann
Dept. of Electrical Engineering

(I) Molecular Beam Epitaxy Growth of II-VI and III-Nitrides (Robert Park)

(a) Widegap II-VI Work

We have continued in this quarter to investigate the use of Sumitomo ZnSe wafers as substrates for widegap II-VI epitaxy.

Hall-effect measurements have been performed in our laboratory on p-type ZnSe:N epilayers grown on the S.I. ZnSe wafers. In order to perform the Hall-effect measurements, we developed a masking and etching procedure to create four mesa contact pads, each comprising the SONY (ZnSe/ZnTe) MQW hole resonant tunnelling structure. The highest room temperature free-hole concentration that we have measured so far in a ZnSe:N/S.I. ZnSe epilayer is $2.1 \times 10^{17} cm^{-3}$. This sample had room temperature and peak mobility values of 21 $cm^2V^{-1}s^{-1}$ and 103 $cm^2V^{-1}s^{-1}$, respectively. By way of comparison, the highest free-hole concentration that we have measured in ZnSe:N/S.I. GaAs epilayers is 4.7×10^{17} cm^{-3} with RT and peak mobility values of 20 $cm^2V^{-1}s^{-1}$ and 120 $cm^2V^{-1}s^{-1}$, respectively. Growth conditions for the ZnSe homoepitaxy have not yet been optimized, however, already the electrical properties of p-type homoepitaxial material are comparable to those of p-type layers grown on GaAs. Free-hole concentration and mobility data are plotted in Figs. I.1 and I.2 as a function of sample temperature for the two p-type epilayers mentioned above (one grown on ZnSe, the other grown on GaAs).

We have also fabricated an etched mesa LED device grown on the ZnSe wafer material which contains a CdZnSe/ZnSe MQW active region as shown in Fig. I.3. The electroluminescence spectrum recorded from the device is shown in Fig. I.4. As can be seen from Fig.I.4, the linewidth of the EL spectrum is only 9.9 nm.

We are in the process of lifetime testing this device together with an identical device structure grown on GaAs and the results of these tests will be reported on in the next quarterly report.

(b) GaN Work

We have continued to refine our process for the growth of unintentionally-doped cubic GaN and Hall-effect measurements on our "best" material reveal room temperature carrier concentration and mobility values of $6 \times 10^{17} cm^{-3}$ and 760 $cm^2V^{-1}s^{-1}$, respectively, together with a peak mobility value recorded at 50K of 11,000 $cm^2V^{-1}s^{-1}$.

We have also performed detailed Hall-effect measurements (particularly at low temperatures) on our Si-doped cubic GaN material and our analysis indicates that impurity band conduction becomes dominant at temperatures below about 70K as evidenced by an increase with decreasing temperatures in the carrier concentration together with a concomitant dramatic reduction in carrier mobility values. This work will be published in the July 4th issue of Applied Physics Letters.

We are currently involved in a carbon doping investigation and we will report on this work in the next quarterly report.

Temperature Dependent Hole Concentration of p-ZnSe/ZnSe and p-ZnSe/GaAs

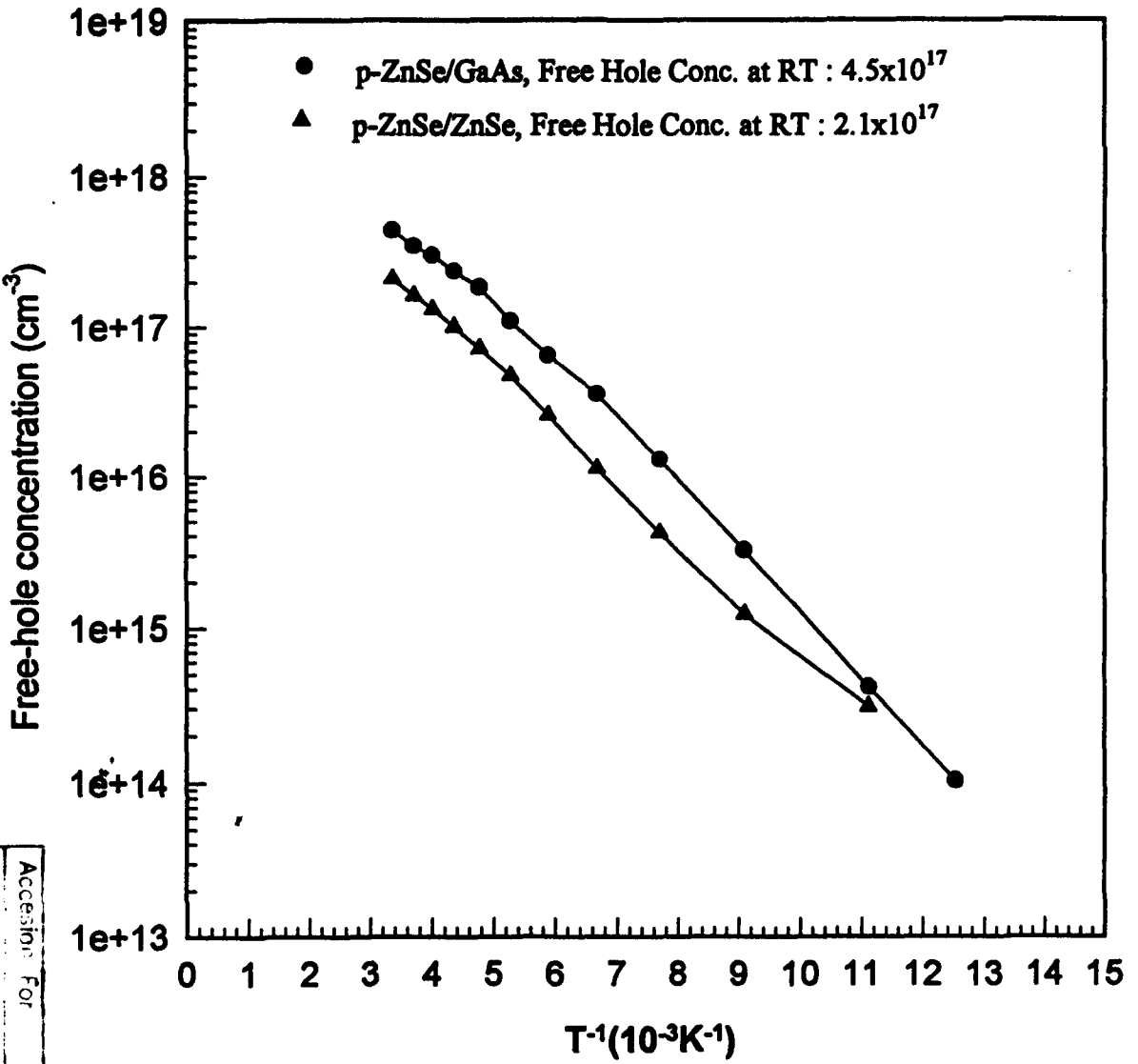

Fig. I.1

Temperature Dependent Hole Mobility of p-ZnSe/ZnSe and p-ZnSe/GaAs

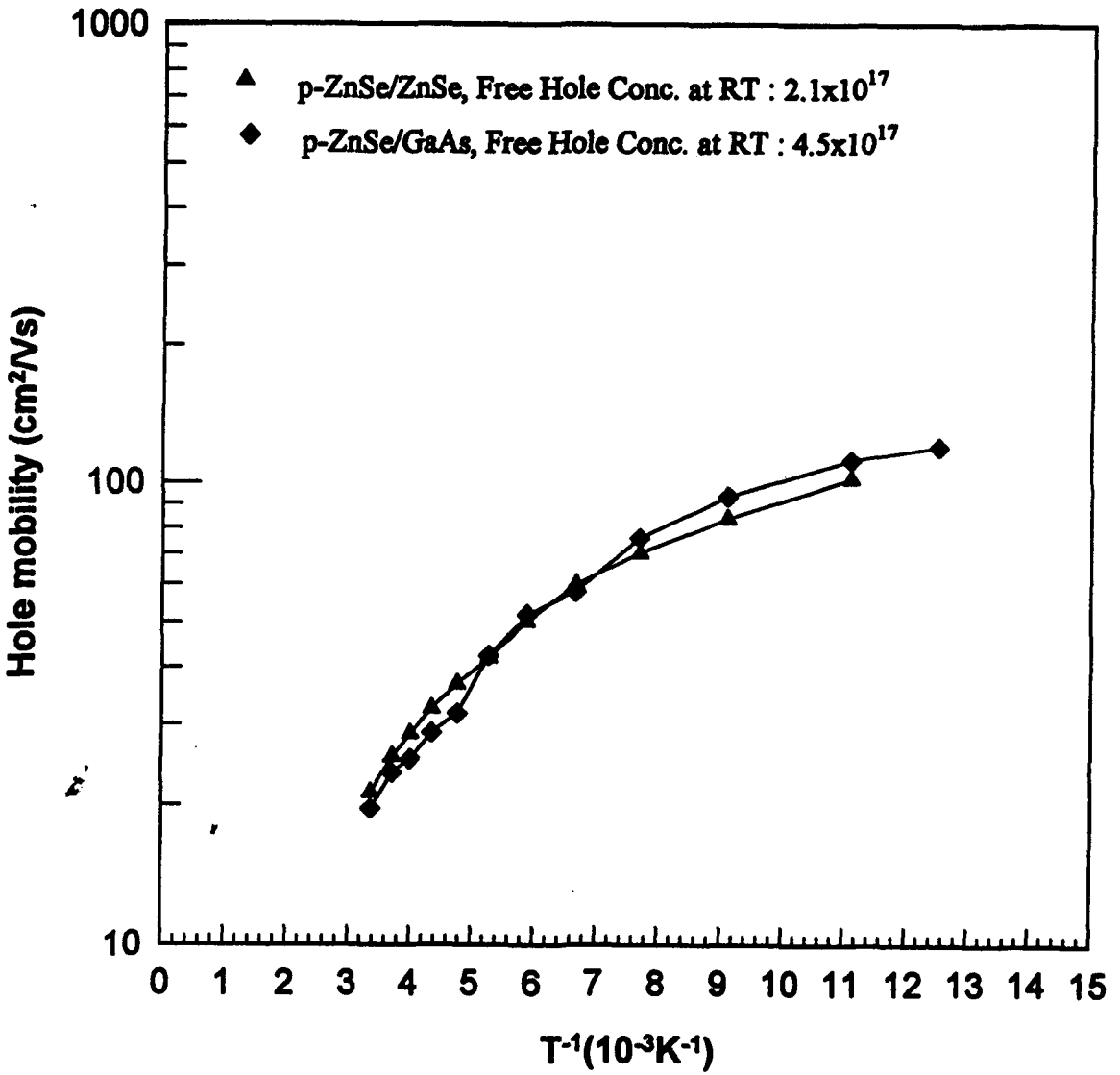

Fig. I.2

$Cd_{0.2}Zn_{0.8}Se$/ZnSe MQW LED grown on ZnSe Wafer

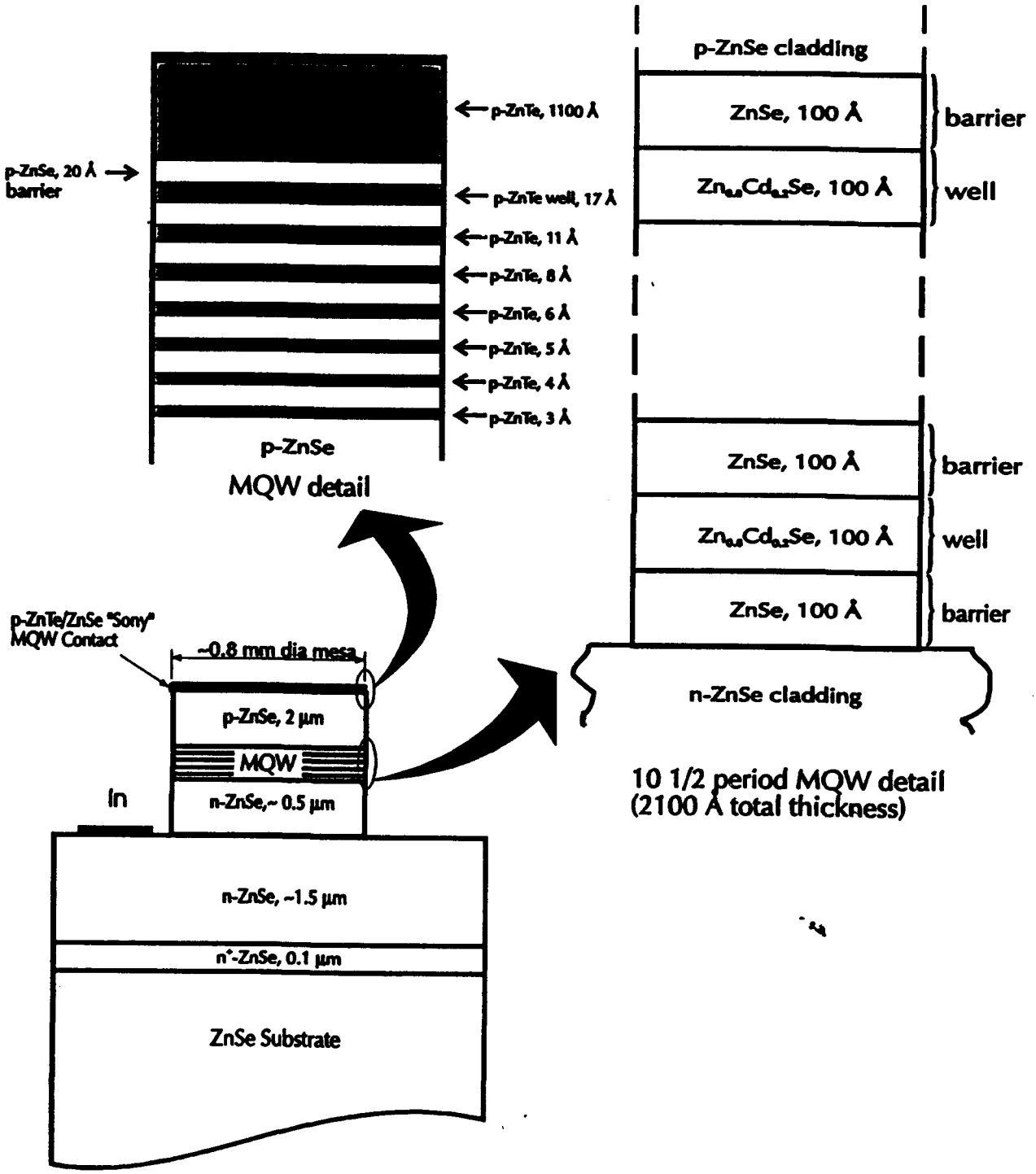

Fig. I.3

$Cd_{0.2}Zn_{0.8}Se/ZnSe$ MQW LED grown on ZnSe Wafer

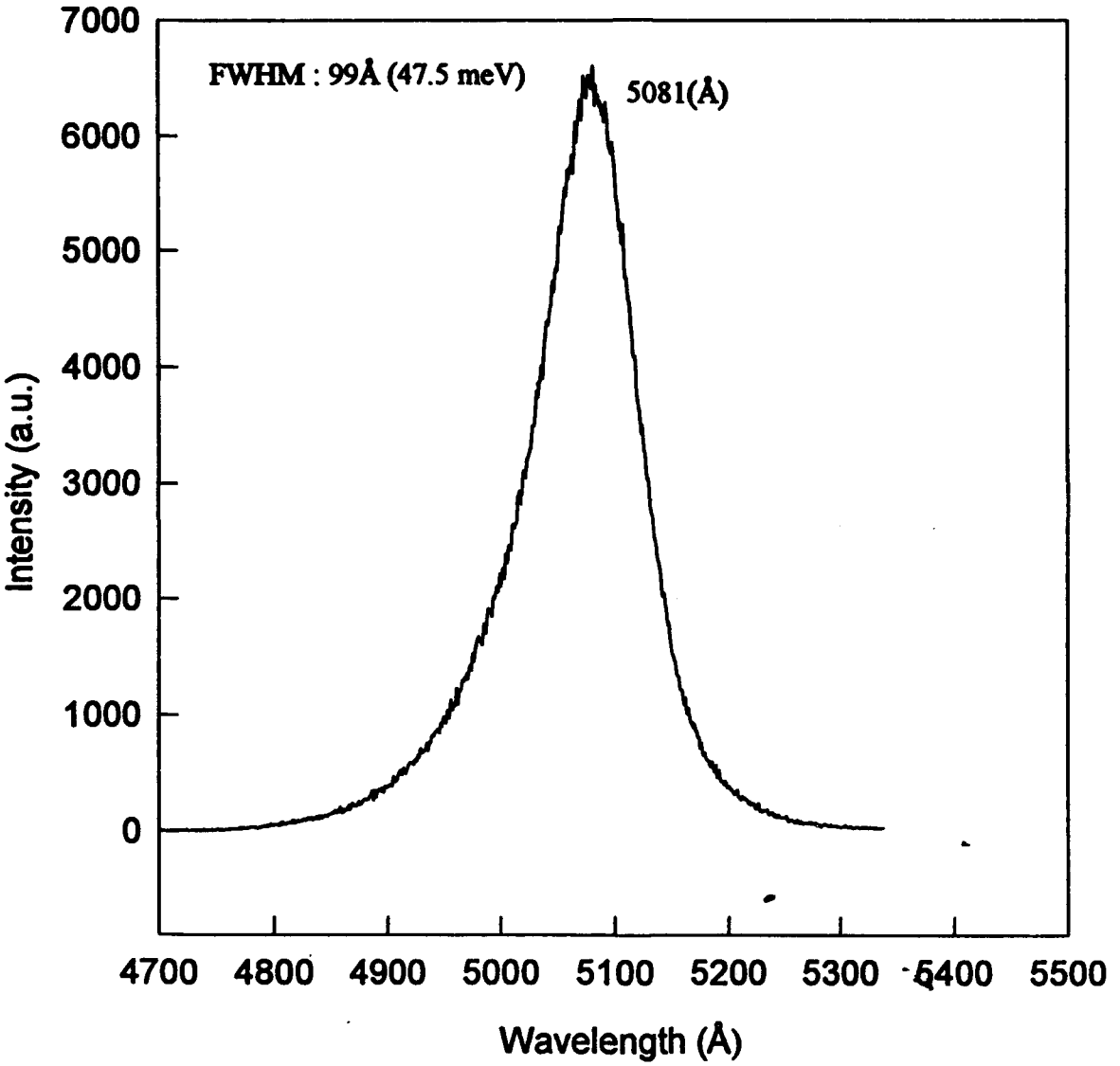

Fig. I.4

(II) Ohmic Contact Formation (Paul Holloway)

Three aspects of ohmic contacts have been studied this quarter: HgSe on p-ZnSe, Au on p-ZnTe, and contacts to GaN. Efforts have focused on identifying the reaction steps occurring during the formation of HgSe contacts from a Se capping layer on p-ZnSe. Based on information in the literature, the amorphous properties of the Se capping layer plays an important role in the formation of HgSe. These properties include the glass transition temperature (T_g) and peak recrystallization temperature (T_c) for Se which are reported to be 30 - 60°C and 110-140°C, respectively. Reaction of the Se layer requires the capped samples to be heated from room temperature to 150°C in the presence of Hg vapor. During this time, Hg to dissolve into the Se capping layer forming a solid solution. This solubility arises due to the open structure of amorphous Se which is comprised of 30-50% Se_8 rings and Se_x polymer like chains. The solubility of Hg in a-Se is in contradiction to the limited solubility predicted for crystalline Se by the Hg-Se binary phase diagram. In the present studies of formation of HgSe contacts, heat treatment at 150°C have been found necessary to form HgSe. This temperature closely corresponds to the values of T_c reported for amorphous Se. Therefore, the amorphous Se layer (containing Hg in solution) is believed to devitrify when heat treatment temperatures reach 150°C, resulting in the precipitation of HgSe and hexagonal Se. TEM analysis has shown that HgSe forms coherent precipitates with the p-ZnSe substrate due to an identical crystal structures and similar lattice parameters. Thus, this study of the reaction process has identified critical parameters which must be characterized in order to optimize contacts formation. These factors include the initial structure of the capping layer, the solubility of Hg in amorphous Se, and the temperature at which devitrification occurs.

With respect to p-ZnTe, work has begun this quarter on a study of ohmic contacts by Au films. The p-ZnTe used for this study were 1100Å overlayers deposited by MBE in the Sony contact scheme for making ohmic contact to p-ZnSe (see section (I) above). Films of Au (1500 Å) have been deposited by DC magnetron sputtering and characterized using current-voltage (I-V) data, Auger electron spectroscopy (AES), and optical and scanning electron microscopy. I-V measurements were performed on the samples as deposited or after annealing at T > 150°C in forming gas for times up to 90 minutes. Linear, low resistance I-V curves were obtained for the annealed samples. An optimum annealing condition of 200°C for 15 minutes yielded a current density of 2 A/cm^2 at 5 V. AES depth profiles have been used to determine interfacial reactions, which appear to be limited. Microscopy shows a planar surface with minor perturbations of morphology by the Au contacts.

An investigaton of ohmic contact formation on n-GaN by reaction of Ti has been undertaken. Thin films of 50 nm of Ti followed by 200 nm of Au were DC magnetron sputter deposited onto intrinsic n-type ($2x10^{18}$ cm^{-3} free electrons), CVD grown, wurtzite GaN. Rectifying contacts were measured for the as deposited films. Upon annealing at 900°C, the contacts show the linear I-V behavior of ohmic contacts with relatively low resistance. Scanning Auger Microscopy (SAM), Secondary Ion Mass Spectrometry (SIMS), and Scanning Electron Microscopy (SEM) were used to characterize the interfacial reaction suspected of giving the ohmic behavior. Thermodynamic data indicate that TiN should form at the interface during the anneal. We have also studied the effects of adding an n-type dopant to the metallization system. We deposited a 100 nm thick layer of Si between the

Ti and Au layers. These contacts, after annealing at 900°C for a few seconds, have demonstrated current-voltage characteristics with a factor 10^2 lower resistance as compared to the annealed Ti/Au contacts. It is postulated that the Si heavily doped the GaN interface during the annealing and reaction step. The interface is being characterized with SAM, SIMS, and SEM. Future work will include testing of these contact schemes for MBE-grown, Si-doped, cubic GaN. The interface reactions at different annealing times and temperatures will be investigated and correlated with contact resistance.

(III) Degradation Mechanism of ZnSe Based Lasers (Kevin Jones)

Thermal Expansion Behavior of Epilayers

A paper entitled, "Thermal Expansion Behavior of ZnSe and $ZnS_{0.03}Se_{0.97}$ Epilayers on GaAs at Temperatures 25 - 250 °C" by J.R.Kim, R.M.Park and K.S.Jones was presented at the MRS spring meeting held in San Francisco, CA in April. While the thermal expansion is accommodated in the perpendicular direction for ZnSe and $ZnS_{0.03}Se_{0.97}$, the in-plane lattice mismatch is not significantly varied as a fuction of temperature. Table 1 shows the relative lattice mismatches between the layer and the substrate in the perpendicular/parallel directions. The coefficient of thermal expansion (CTE) was obtained and is shown in Figure III.1. The values of the CTE's are slightly higher than the previously reported values.

Defects Generation in the Active Region

Experiments are in progress to study the susceptibility to point defect generation around the quantum well by electron beam irradiation in TEM, and to study the influence of structural defects on diffusion in the region of the active layer by comparing SIMS profiles before and after annealing.

Table 1. Relative Lattice Mismatches in the perpendicular/parallel directions(ppm)

Temperature	n-type ZnSe	p-type ZnSe	n-type ZnSSe	p-type ZnSSe
R.T.	2300/2600	2500/2700	200/ 10	200 / 50
100 °C	2700/2600	2900/3000	600/ 10	800 / 50
250 °C	3600/2400	3700/3000	1400/ 10	1500 / 50

(IV) Modelling of the Hall Effect Data from n-ZnSe (J.H. Simmons)

Hall effect data yield free carrier concentrations and free carrier mobilities as a function of temperature for samples with varied dopant concentrations. In n-ZnSe films prepared by Park and Rouleau, free carrier concentrations near 10^{19} cm^{-3} were achieved therefore a broad range of dopant concentrations were available for the study. The

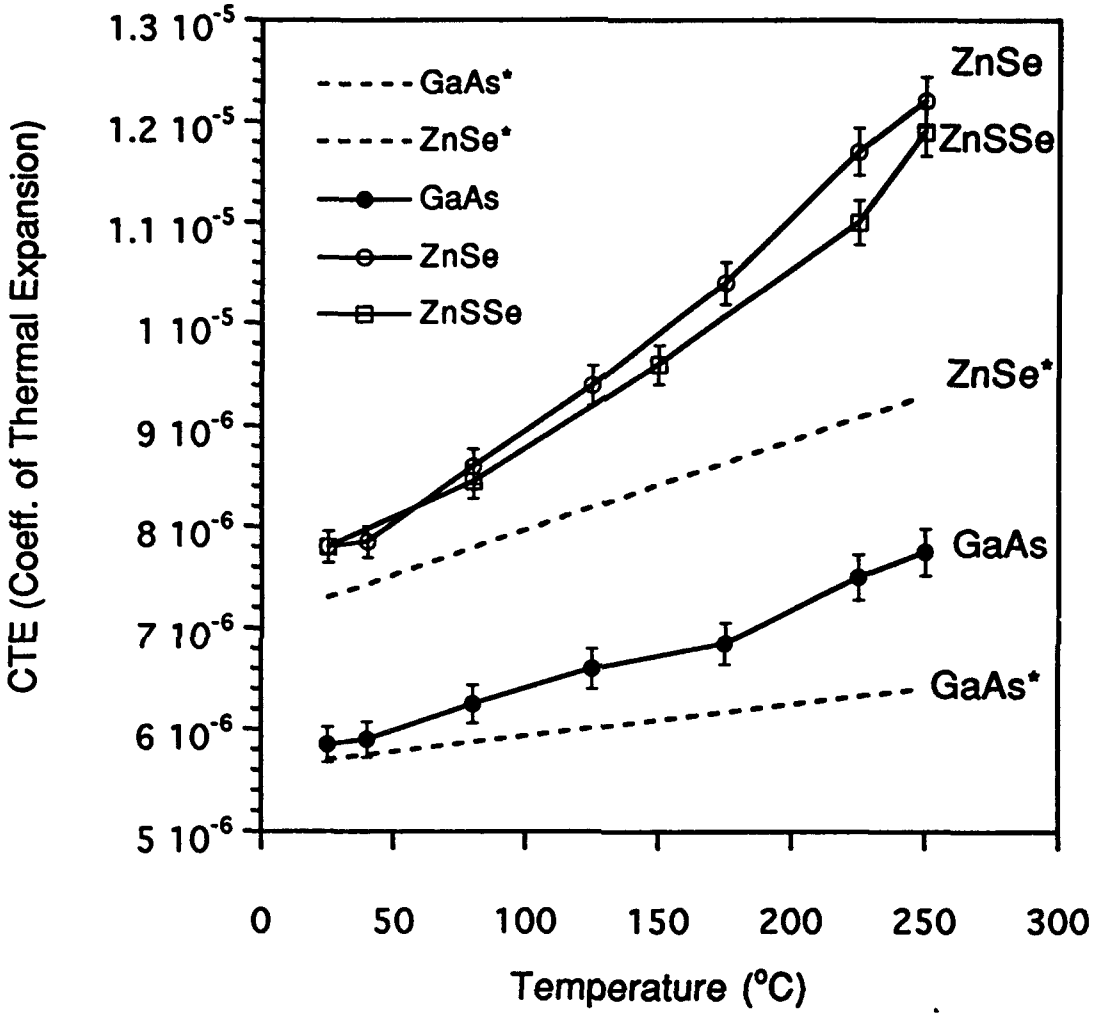

Fig. III.1 CTE at Various Temperatures

* Previously reported values

temperature dependence of free carrier concentration and mobility for 6 samples is shown in Figures IV.1 and IV.2. In Figure IV.1, the free carrier behavior of the two lowest concentration samples (Samples 1 [open circles] and 2 [filled circles]) exhibits the temperature dependence expected of the typical freeze-out process observed in semiconductors, whereby a decrease in temperature reduces the concentration of ionized donors, and consequently the free carrier concentration. The behavior of the two heavily-doped samples (Samples 5 [open squares] and 6 [filled squares]) is typical of metallic behavior in which the Fermi energy has risen above the bottom of the conduction band. The behavior of the intermediate samples (Samples 3 [open triangles] and 4 [filled triangles]) has not been adequately modelled previously. While various theories have been proposed to explain the transition from semiconducting to metallic behavior, there has been a lack of agreement between experiment and theory.

We have developed several approaches to model the transition from semiconducting to metallic behavior and have discovered that, in general, several of the proposed approaches will describe adequately the variation of the free carrier concentration with temperature. However, they do not adequately account for the free carrier mobility. Therefore, any attempt at model development had to fit both the free carrier concentration and mobility.

In our early studies, we examined the Mott theory of an upper and lower Hubbard band, and were able to fit the free carrier concentration but not the mobility. This data was presented last year. This year, we have examined all the components in the free carrier equation and discovered that the behavior of the intermediate samples (3 and 4) could be best described assuming a process of carrier tunnelling between isolated impurity levels. The model required that a distribution of impurity level energies be present, so that only a fraction of the bound carriers could tunnel. This was first postulated by Anderson and is known as an Anderson transition. This approach has been very successful in describing all the free carrier concentration data and the mobility data of n-ZnSe. The lines drawn in Figure IV.1 and IV.2 represent the Anderson transition model derived by us. It is clear that they fit the data extremely well. To our knowledge, this is the first direct observation of an Anderson transition in semiconductors.

Briefly, the model we are using assumes the following scenario:

(1) At room temperature and above, free carriers are formed by thermal ionization of donor states.

(2) Below room temperature, the concentration of ionized states decreases while the concentration of bound impurity states increases. In the presence of compensation, a second source of conduction appears as a fraction of bound impurity states allow tunnelling between states. This tunnelling only involves a *fraction* of the bound carriers. This fraction is dependent on doping level and increases at higher doping levels.

(3) When the Bohr diameter of the donor levels is of the order of the donor-to-donor distance, the impurity levels form an impurity band in which the carriers are free to contribute to conduction. Samples 5 and 6 exhibit a temperature-independent free carrier concentration because all the donors contribute to conduction whether through free carriers or donor band conduction. The model also assumes a different mobility in the conduction and in the impurity band. The model thus obtained has been fitted to the free carrier concentration and to the mobility dependence on temperature for all the samples measured. A paper on this result is in preparation.

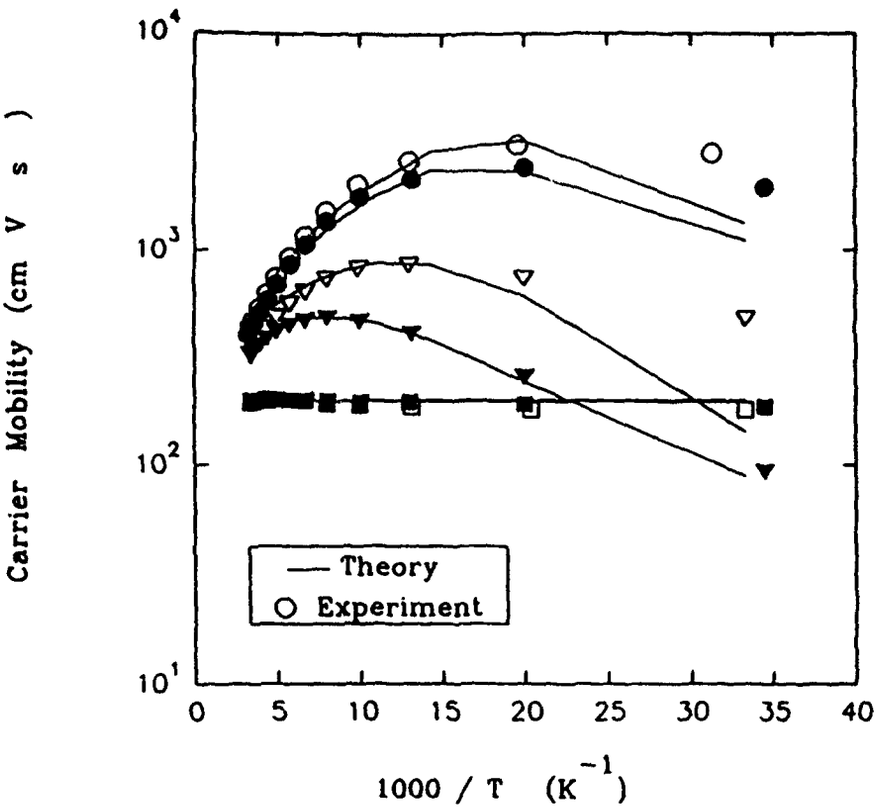

Fig. IV.2

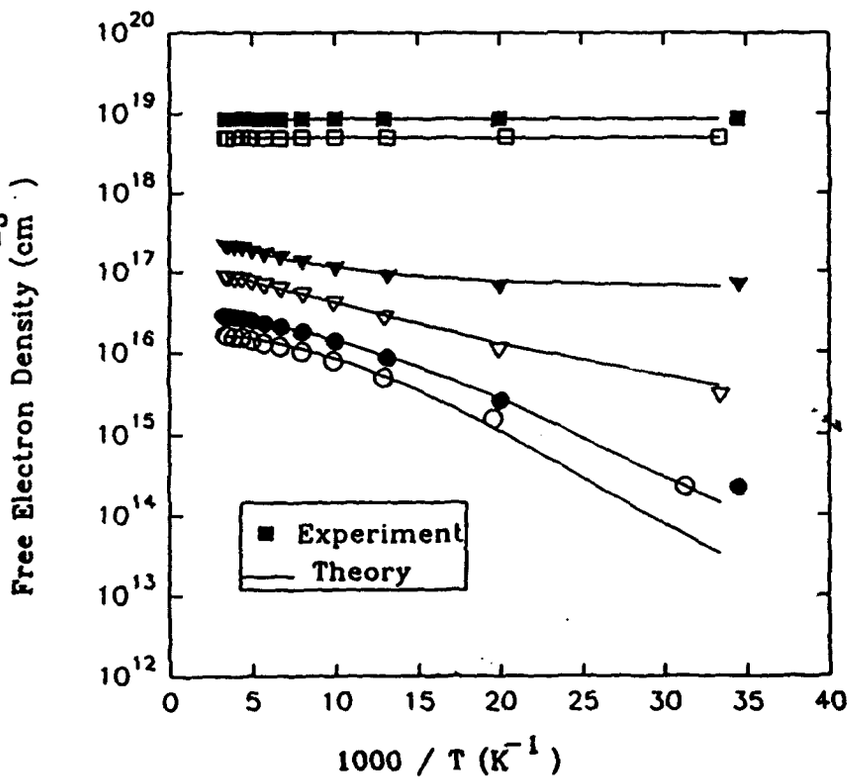

Fig. IV.1

(V) Tim Anderson

From the last report, studies indicate that better quality ZnCdS is grown at the higher end of the growth temperature range of 250 to 450°C for the various orientation GaAs substrates. Further studies indicate that the best growth temperature is 550°C. At that temperature, the FWHM from HRXRD of ZnCdS grown on (111) substrates is 550 arc-seconds. This is the lowest reported to date in the literature using this precursor combination. For those films grown on the (100) substrates, the FWHM averages around 1000 arc-seconds but of poor quality in comparison to films grown on the (111) substrates. This large FWHM is due to the high density of stacking faults in the <111> direction when ZnCdS is grown on the (100) substrates. By depositing on the (111) surface, the stacking fault density is minimized, but not eliminated.

To further improve the crystalline quality of the ZnCdS epilayers, a ZnSe buffer layer was grown prior to the growth of ZnCdS. The X-ray results show a degradation of quality with the buffer layer. In future work, we will shift to methyl mercaptan as a S source in an attempt to reduce the stocking fault density. There is a report in the literature that this precursor produces considerable improved structural quality in sulfides.

With these results, doping with Ga and Al was performed using triethylgallium (TeGa) and triethylaluminum (TEAl) to achieve n-type character. The TEAl does not crack well for growth temperatures of 550°C. At the best growth conditions, the maximum free carrier concentration achieved was $10^{15}/cm^3$. More studies will be done at higher growth temperatures to enhance the cracking of TEAl and increase Al incorporation. The free carrier concentrations were determined by Hall measurements. Again with the best growth condition, preliminary studies show that the maximum free carrier concentrations with Ga doping is $10^{14}/cm^3$. Since TEGa cracks at much lower temperatures than TEAl, it may be a better dopant source than TEAl in consideration of the relatively low growth temperature. SIMS analysis will be performed on these samples to determine quantitatively the concentration of dopants.

Work has also bee initiated on the growth of GaN on (0001) and (0112) sapphire and (0001) 6H-SiC substrates using TeGa and NH_3 precursors. A two-step growth procedure was adopted in which a thin low temperature GaN is first grown, followed by the growth of a thicker GaN film at higher temperature (850°C). X-ray diffraction and Raman scattering measurements indicates growth of single phase wurtzite GaN. The quality of the films was found to improve with increasing III molar rata and decreasing nitridation times. A series of substrates are in the process of being patterned with Pt, N, TiC and SiO_2. These mask materials are known catalysts for the thermal decomposition of NH_3 and will be tested for the selective area growth of GaN.

(VI) Development of Diode Lasers (Peter Zory)

(a) Photopumping

Tunable wavelength photopumping experiments using the nitrogen laser pumped dye laser continue using ZnSe, GaN and CdZnS samples provided by Drs. Park and Anderson.

(b) Diode Pumping/Reliability

Three CdZnSe quantum well epitaxial wafers have been received from 3M for use in degradation studies. Wafers will be processed into LED devices with thin gold contacts and degraded "appropriately" using a TV defect viewing system. TEM samples will be prepared from these degraded devices by Dr. Jones and students with the goal of determining the nature of the defects causing rapid degradation of the CdZnSe light emitters.

(VII) Theoretical Calculations of Dopants of ZnSe (Gertrude Neumark)

One high-priority objective of this work is to establish whether present growth/doping techniques lead basically to quasi-equilibrium or non-equilibrium nitrogen acceptor incorporation: if it is the former, attendant strong compensation would be concluded to be unavoidable. Since present experimental indications are that there is strong compensation, another high-priority objective is to determine which compensating species are likely, and (if possible) means to avoid them. For both of these objectives, information on ion and defect mobilities is important. It can be noted that a deep donor in heavily N doped ZnSe appears to be quit mobile, based on a decreasing net acceptor density with time reported by Hauksson et al. [Appl. Phys. Lett. 61, 2208 (1992)]. This conclusion is also consistent with evidence of preferential donor-acceptor pairing for this species (Radomsky and Neumark, abstract submitted to SPIE) since such pairing can be observed only in the case of high ion mobilities. In this connection, the recent suggestion [Bowers et al., J. Electr. Mat. 23, 251 (1994)] that the N acceptor species is interstitial N is also of interest. It is well-known that interstitial species tend to be very mobile.

We have concluded that it would thus be of high interest to determine whether acceptor N is, indeed, likely to be interstitial. The argument given for assuming N to be interstitial is an interpretation of data which leads to a temperature dependent activation energy. However, it is well-known that activation energies can be temperature dependent due to screening [the theory is given by Neumark, Phys. Rev. B 5, 408 (1972)]. We will therefore compare the literature results to the theory. If the data can be explained by screening, there is no need to assume that N acceptors are interstitial.

(VIII) MOCVD Growth of GaN (Jacques Pankove)

Our objective is to grow pn junctions in GaN that will be the basis for short wavelength emitters and lasers. In the past quarter, the quality of undoped GaN films was improved further, especially for the runs in the second deposition system (a horizontal cold-wall MOCVD system). The electron mobility at room temperature was increased to 154 cm^2/V-sec, and the free electron concentration is in the low 10^{18} cm^{-3}. The cathodoluminescence spectra of the films exhibit a sharp edge exciton luminescence at 3.40 eV (see Fig. VIII.1). The improvement is a result of a better optimized buffer layer. In many of the recent runs, SEM picture showed relatively large hexagonal crystals (20 μm to 50 μm in diameter--see Fig. VIII.2). We also started p-type doping studies using the second system. The Mg-doped films are specularly clear but still insulating. In the near

Fig. VIII.1 Cathodoluminescence spectrum of a GaN film grown on basal plane sapphire (Room Temperature).

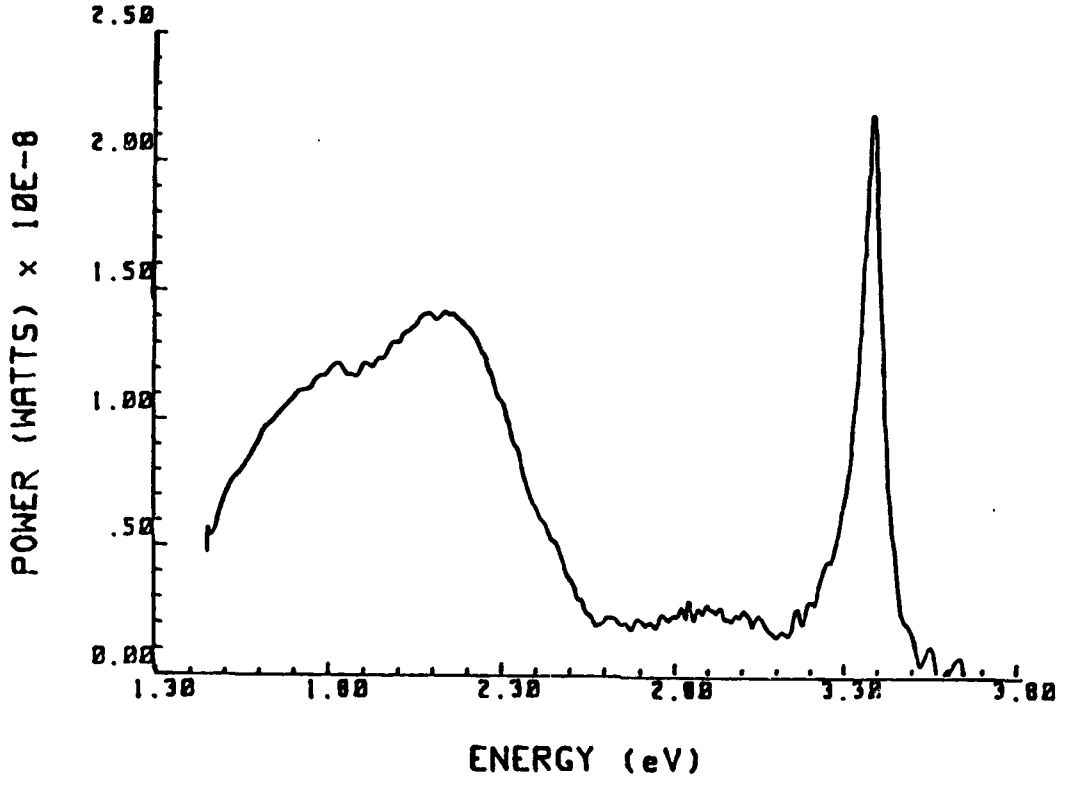

Fig. VIII.2 SEM micrograph of GaN on basal plane sapphire, showing crystal grains 50μm across (720x magnification).

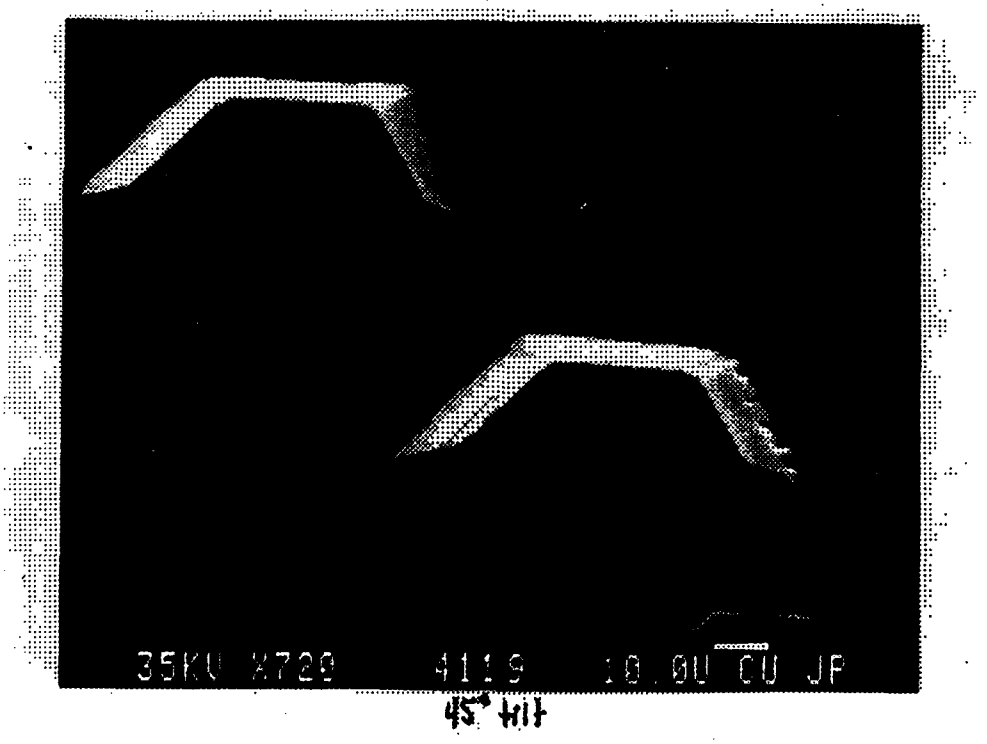

future, the buffer layer will be further optimized, and the flow rate of cp_2Mg will be increased.

(IX) Gain Modeling in II-VI Strained-Layer QW Structures (Reinhart Engelmann)

In a Separate Confinement Heterostructure (SCH) Single Quantum Well (SQW) structure, as the injection level becomes increasingly higher, quasi-Fermi levels are raised and carrier distributions in the barriers will increase. This carrier spill-over may become significant, especially in diode lasers operating at high temperature or in laser structures with low band offsets (poor carrier confinement). Generally, due to the structural difference between conduction and valence band (e.g. electron-to-hole effective mass ratio is about 1/6 in ZnCdSe/ZnSSe based lasers), the spill-over of electrons and holes tend to be different. This will result in an internal electrostatic field which works to reduce the difference of the electron and hole distributions, leading to a modification of the band profile. It is still necessary to evaluate this injection-induced electrostatic confinement effect in gain/threshold current calculations for device design and optimization. Also, the quantitative modeling of this effect can help in gaining a better understanding of the influence that the band offset ratio, $Q_c = \Delta E_c/(\Delta E_c + \Delta E_v)$, has on device performance. Values for Q_c are currently still very difficult to predict. We developed a comprehensive band filling model for a SCH SQW laser structure which including the spill-over carriers contribution.

Model for Injection-Induced Electrostatic Carrier Confinement.

The numerical method is based on solving the coupled set of Poisson and Schroedinger equations. [The original Schroedinger/Poisson solver (SPS) for HEMT is courtesy of Claus Fischer, Technical University Vienna, Austria.] The solutions of the above problem are similar to those applied in HEMT (high-electron-mobility transistor) simulations, except now both electrons and holes need to be considered at the same time. The solution of Poisson's equation is based on a standard finite difference method. The solution of Schroedinger's equation follows the Numerov process as described by P. C. Chow. [P. C. Chow, Amer. J. Phys., vol. 40, pp. 730-734, May 1972] The band profile and carrier distributions are then obtained by self-consistent iteration procedures.

As an example, we consider a particular device structure (SCH SQW $Cd_{0.2}Zn_{0.8}Se/ZnS_{0.06}Se_{0.94}$, 6.5 nm QW, 100 nm barrier) to perform our numerical calculations. The injection levels is about $5x10^{18}$ cm^{-3} which is close to the threshold carrier density measured in the experiments. The initial band configuration is shown in Fig. IX.1a, as estimated from strain effect and common anion rule. The $Q_{c,v}$ value (referred to the heavy hole band-edge) in this case is about 0.62. As we keep the total charge neutrality in the combined barrier and QW region, the locally unbalanced carrier distribution at this injection level is shown in Fig. IX.1c, where in this particular case there are more electrons in the QW and more holes in the two barriers. The modification of the band profile due to the locally unbalanced carrier distribution is obtained with the comprehensive model as shown in Fig. IX.1b. The injection induced carrier confinement can be clearly observed when comparing with the balanced carrier distribution shown in Fig. IX.1d.

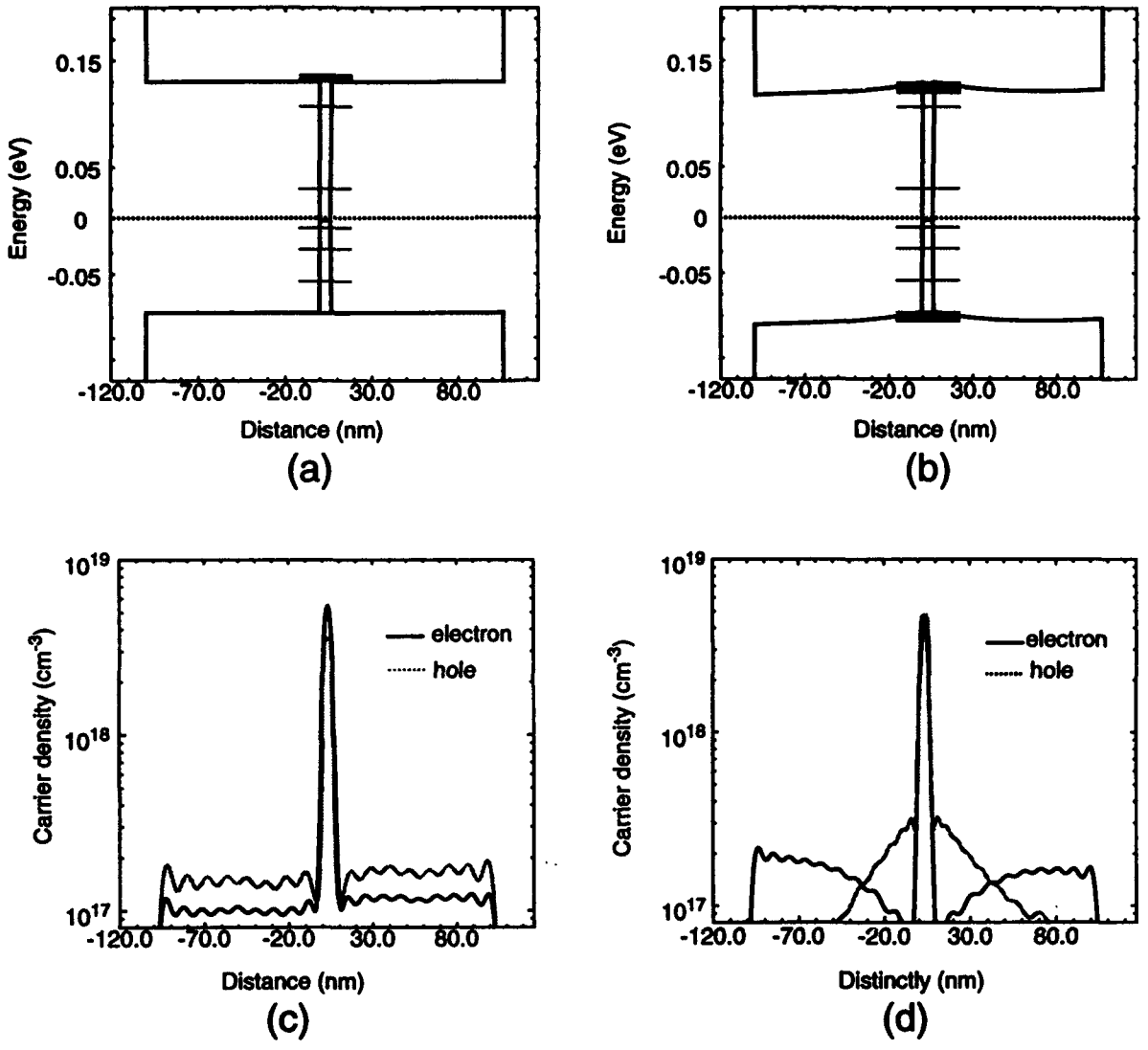

Fig. IX.1 Band profile (without QW band gap) and carrier distribution. (a) initial band diagram, (b) band diagram including injection induced carrier confinement, (c) unbalanced carrier distribution of configuration (a), (d) balanced carrier distribution of configuration (b).

In summary, we have developed a comprehensive theoretical approach to analyze the injection induced carrier confinement and its influence on the band filling process of SCH SQW lasers. An accurate picture of carrier distributions can be obtained from this comprehensive model.

Future plans for the above band filling model will be combined with the gain/ threshold-current-density calculations. Also, doping effects and ionization will be considered. The field ionization (Frankel - Poole effect) will be incorporated into the model to simulate the hole freeze-out.

Presentations this quarter

- R.M. Park, "Development of wide-bandgap semiconductors for short-wavelengt diode laser applications," **Invited Physics Colloquium**, University of South Florida Tampa, FL, March 4, 1994.

- P.S. Zory, "Blue-Green Diode Laser Overview" **Invited Presentation**, DOD/DOE sponsored Diode Laser Technology Conference in Fort Walton Beach, Fl on 21 April 94.

- P.S. Zory taught course on "Visible Semiconductor Lasers" and organized and chaired session on Blue-Green Diode Lasers at the OSA/IEEE sponsored Conference on Laser and Electro-Optics (CLEO) in Anaheim, CA 10, 12 May 94.

- P.S. Zory, **Invited Discussion** of the relative merits of II-VI and III-V wide bandgap light emitters at the Eleventh Annual, IEEE/LEOS sponsored Semiconductor Laser Workshop in Anaheim, CA on 13 May 94.

- Y. Cai and R. Engelmann, "Reduction of threshold current density of CdZnSe/MgZnSSe blue-green quantum well diode lasers", CLEO'94, Anaheim, CA, May 1994, paper CWH24

- Y. Cai and R. Engelmann, "Numerical modeling of injection induced carrier confinement in quantum well (QW) structures", 3rd Intern. Workshop on Computational Electronics, Portland, OR, May 1994, paper FriP3

- P.H. Holloway, T.-J. Kim, V. Fischer, P. Viljoen, W. Lampert, T.W. Haas, and J. Woodall, "Regrowth of GaAs during reactions with contact metallization and the consequence on formation of ohmic contacts", **INVITED LECTURE**, Materials Research Society 1994 Spring Meeting, San Francisco, CA, April 4-8, 1994.

- J. Fijol and P.H. Holloway, "Low resistance electrical contacts to N-doped ZnSe by ex situ growth of HgSe", Materials Research Society Spring Meeting, San Francisco, CA, April 4-8, 1994.

Papers during quarter

- J.G. Kim, A.C. Frenkel, H. Liu and R.M. Park, "Growth by MBE and electrical characterization of Si-doped zincblende GaN films deposited on β-SiC coated (001) Si substrates." To be published in the July 4th issue of Applied Physics Letters.

- Y. Cai and R. Engelmann, "Design Optimization for ZnCdSe/MgZnSSe Blue Green Quantum Well (QW) Diode Lasers," Proceedings of the Oregon Academy of Science, Vol. XXX, Oregon State University, Corvallis, OR, 1994 (52nd Annual Meeting of OAS, 26 Feb 1994), p.60.

- V. Fischer, P.H. Holloway, P.E. Viljoen, W.V. Lampert, T.W. Haas, and J.M. Woodall, "Regrowth of GaAs during reactions with contact metallization and the consequence on formation of ohmic contacts", in Advanced Metallization for Devices and Circuits-Science, Technology and Manufacturability, Ed. by S.P. Murarka, A. Katz, K.N. Tu, and K. Maex (MRS, Pittsburgh, PA, 1995) Vol. 337, in press.

Post Doctoral Associates, Graduate Research Assistants, and Undergraduate Research Assistants:

Post Doctoral Associates:

Chang H. Qiu with Dr. Pankove

Graduate Research Assistants:

Bruce Liu with Dr. Park
Austin Frenkel with Dr. Park
George Kim with Dr. Park
Y.S. Park with Dr. Zory
C.L. Young with Dr. Zory
C.F. Hsu with Dr. Zory
Igor Kuskovskiy with Dr. Neumark
Li Wang with Dr. Simmons
Y. Cai with Dr. Engelmann
Charles Hoggatt with Dr. Pankove
William A. Melton with Dr. Pankove
John Fijol with Dr. Holloway
Jeff Trexler with Dr. Holloway
Steve Miller with Dr. Holloway
Eric Bretschneider with Dr. Anderson
Joe Cho with Dr. Anderson
J. Kim with Dr. Jones
S. Bharatan with Dr. Jones

Undergraduate Research Assistants:

Julie Sauer with Dr. Simmons
Greg Darby with Dr. Park
Bob Covington with Dr. Anderson
Michael Mui with Dr. Anderson
Brendon Cornwell with Dr. Anderson